

LETTER TO THE EDITOR

# Low-lying magnetic loops in the solar internetwork

M. J. Martínez González<sup>1,2</sup>, M. Collados<sup>2</sup>, B. Ruiz Cobo<sup>2</sup> and S. K. Solanki<sup>3</sup>

<sup>1</sup> LERMA, Observatoire de Paris-Meudon, 5 place Jules Janssen, 92195 Meudon, France  
e-mail: Marian.Martinez@obspm.fr

<sup>2</sup> Instituto de Astrofísica de Canarias, Vía Láctea S/N, 31200 La Laguna, Spain  
e-mail: mcv@iac.es, brc@iac.es

<sup>3</sup> Max-Planck-Institut für Sonnensystemforschung, Max-Planck-Str. 2, 37191 Katlenburg-Lindau, Germany  
e-mail: solanki@mps.mpg.de

## ABSTRACT

*Aims.* The aim of this work is to study the structure of the magnetic field vector in the internetwork and search for the presence of small-scale loops.

*Methods.* We invert  $1.56\ \mu\text{m}$  spectropolarimetric observations of internetwork regions at disc centre by applying the SIR code. This allows us to recover the atmospheric parameters that play a role in the formation of these spectral lines. We are mainly interested in the structure of the magnetic field vector.

*Results.* We find that many opposite polarity elements of the internetwork are connected by short ( $2 - 6''$ ), low-lying (photospheric) loops. These loops connect at least the 10 – 20 % of the internetwork flux visible in our data. Also we have some evidence that points towards a dynamic scenario which can be produced by the emergence of internetwork magnetic flux.

**Key words.** Sun: magnetic fields — Sun: atmosphere — Polarization — Methods: observational

## 1. Introduction

Magnetic fields appear on the solar surface in the form of bipolar regions, with the two polarities connected by magnetic field lines in the shape of loops. If the loops are sufficiently large they are traced in  $H\alpha$  (arch filament systems) or EUV or X-ray images (transition region and coronal loops). There is also mounting evidence for the presence of myriads of small loop-like structures in the upper quiet atmosphere (e. g. Feldman et al., 1999) and in the photosphere (Lites et al., 1996; de Pontieu, 2002), and the presence of such loops has been invoked by the complex mixture of magnetic polarities typical of the quiet Sun. Direct measurements of the full magnetic structure of a loop are extremely rare, being basically restricted to chromospheric loops in emerging flux regions (Solanki et al., 2003). Here we trace the field of low-lying loops and present evidence that they are common in the internetwork quiet Sun.

Our knowledge of the magnetic field in the internetwork has evolved rapidly in recent years. The magnetic features present in internetwork regions, as seen by the Zeeman effect, are unresolved, occupy a very small portion of the resolution element (1 – 2 %) and have field strengths of a few hundred G (Keller et al., 1994; Lin, 1995; Lin & Rimmele, 1999; Khomenko et al., 2003; López Ariste et al., 2006b; Martínez González et al., 2007; Asensio Ramos et al., 2007a). Probably the rest of the resolution element is filled by magnetic fields that currently are only detectable by means of the Hanle effect (Stenflo, 1987) or the Zeeman sensitive  $\text{Mn I}$  line at  $1.52\ \mu\text{m}$  (Asensio Ramos et al., 2007a). If we assume that such a hidden magnetic field is tangled at subresolution scales and that it occupies the whole resolution element, the most sophisticated Hanle effect determinations measure a mean magnetic field of

100 G (Trujillo Bueno et al., 2004) while previous estimates give a much weaker field (Faubert et al., 2001). In this type of studies, the spatial resolution is given by the slit length, since the signal is averaged over the whole slit in order to obtain an adequate signal to noise ratio. In addition, some works find empirical evidence of this tangled nature (Stenflo, 1987; Manso Sainz et al., 2004; Asensio Ramos et al., 2007a). The present paper extends the knowledge of the quiet Sun by revealing the connectivity of magnetic features in the internetwork and partly its three dimensional structure.

## 2. Observations and data reduction

The observational data consist of two scans of quiet Sun regions. One of them was located at disc centre and the other one at  $\mu = 0.88$ . They were observed on the 29th and the 30th of July 2000, respectively. All four Stokes parameters of the pair of  $\text{Fe I}$  lines at  $1.56\ \mu\text{m}$  were recorded using the Tenerife Infrared Polarimeter (Collados, 1999) installed at the Vacuum Tower Telescope at El Teide observatory. In both cases, the integration time at each slit position was 1 min which allowed us to achieve a noise level in the polarization profiles of  $4.1 \times 10^{-4} I_c$  in the observation at disc centre and  $2.5 \times 10^{-4} I_c$  in the one at  $\mu = 0.88$ . Here,  $I_c$  is the continuum intensity. In Fig. 1, the  $I_c$  maps are shown for both scanned areas. The slit was oriented vertically and scanned horizontally. We used a correlation tracker (Ballesteros et al., 1996; Schmidt & Kentischer, 1995) to correct for image motions due to the seeing. The continuum intensity contrast of both data sets is 1.4 % and 2.0 %, respectively, for the maps at  $\mu = 0.88$  and  $\mu = 1$ . In both maps, the granulation pattern is clear and the spatial resolution was estimated to be of the order of  $1''$ . This was computed using the Fourier transform of the  $I_c$  images and choosing the frequency where the power

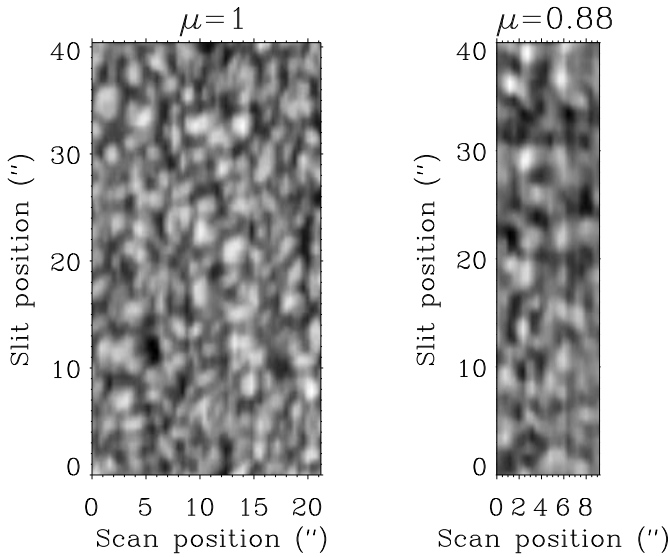


**Fig. 1.** Continuum maps of the observations taken at disc centre (left) and at  $\mu = 0.88$  (right).

was 10 times above noise. In both cases the pixel size, the slit width and the scan step were all  $0.4''$ .

The standard reduction of the data included dark current and flatfield corrections. The polarimetric calibration was performed with the aid of polarization optics of known properties, located at an appropriate place in the optical path. Any residual crosstalk between the Stokes parameters, because of the uncalibrated coelostat mirrors, were removed using statistical techniques described in Collados (2003). After that, a statistical procedure called Principal Components Analysis (PCA) was applied to reduce the noise level of the polarization profiles. This consists in creating a basis with the eigenvectors of the correlation matrix of the observations in which they can be represented. Then we can eliminate from the basis those eigenprofiles that have no information about the real signals and are dominated by noise and reconstruct the observations with this shortened base. This is feasible because of the fast decrease of the eigenvalues and allows us to increase the noise level of the observations.

After denoising with PCA, the noise level of Stokes V is  $6.5 \times 10^{-5} I_c$  and  $9.0 \times 10^{-5} I_c$  for the observations at  $\mu = 1$  and  $\mu = 0.88$ , respectively. Stokes Q has a noise level of  $1.1 \times 10^{-4} I_c$  and  $8.5 \times 10^{-5} I_c$  and Stokes U  $2.0 \times 10^{-4} I_c$  and  $5.0 \times 10^{-5} I_c$  at disc centre and at  $\mu = 0.88$ , respectively.

### 3. Analysis of the data

We obtain the magnetic field vector by inverting the four Stokes profiles using the SIR<sup>1</sup> code (Ruiz Cobo & del Toro Iniesta, 1992). We perform a two component inversion based on a magnetic atmosphere that occupies a fraction of the resolution element and a field free one filling the rest of the space. Including two components in the inversion increases the number of free parameters. Then, in order to end up with an adequate number of degrees of freedom (see Asensio Ramos et al., 2007b) we chose the majority of the variables to be constant with height. The microturbulent velocity in both components, the line of sight flow velocity of the magnetic component, the magnetic field strength and the azimuth of the magnetic field vector are assumed to be

constant with height. The macroturbulent velocity is forced to be the same in both atmospheres. The macroscopic velocity of the non magnetic atmosphere has 3 nodes and the inclination of the magnetic field vector has 2 nodes. The temperature stratification of each atmosphere was allowed to vary independently with 5 nodes.

In Fig. 2 we show the maps of the amplitude of circular polarization for both scans. Superimposed to them, some contours of equal amplitude of linear polarization ( $\sqrt{A_Q^2 + A_U^2}$ ) are plotted ( $A_Q$  and  $A_U$  represent the maximum absolute amplitude of the Stokes  $Q$  and  $U$  profiles). In both maps there are numerous examples of a linear polarization signal lying in between two opposite polarity circular polarization signals. Small low-lying magnetic loops are expected to show just such a signature: the magnetic field vector points up on one side of the structure, is horizontal in the middle and points down on the other side. We found 6 clear cases of such structures in the map at disc centre and 5 in the map at  $\mu = 0.88$ . They are enclosed by the white rectangles in Fig. 2. In the examples in the  $\mu = 0.88$  map all the linear polarization is slightly displaced towards one of the circular polarization signals. In the disc centre map this is not a systematic behaviour. It might be a projection effect or the foot points having different field strengths.

We discuss now in detail the results from inversions of the clearest loop identified by the thick dashed-line rectangle in the observation at  $\mu = 0.88$  (the others show similar properties and geometries). The inclination and azimuth of the magnetic field vector recovered from the inversions in the line-of-sight reference frame are transformed to the local reference frame (without solving the  $180^\circ$  degrees azimuth ambiguity).

In the left panel of Fig. 3, the horizontal component of the magnetic flux vector is presented together with the vertical magnetic flux density for the thick dashed rectangle in Fig. 2. The white lines in the left panel of Fig. 3 represent the direction of the magnetic field vector. The values of the background flux density clearly correspond to internetwork regions in all the pixels containing the loop-like structure. The horizontal component of the magnetic field vector in the pixels in between the two opposite polarities is approximately directed along the line that joins them. In the central and right panels of Fig. 3, we plot the magnetic field lines on a vertical cut through the atmosphere along the line joining the two polarities. The vertical magnetic flux density is indicated by the colour scale and the superimposed arrows represent the magnetic field vectors. The azimuth values differ by  $180^\circ$  in the two panels, both solutions being consistent with the observed spectral profiles. Note that the inclination of the magnetic field vector is nearly height independent even if we allow it to vary. The magnetic field lines have been computed as those lines that are parallel to the vector field. In each slit position in centre and right panels the geometrical heights have been displaced to have the same gas pressure at  $h=0$ . The reference gas pressure value is the mean value at  $h=0$ . The applied displacements are small, having a mean value of 20.5 km. The  $\Omega$ -loop (centre) or U-loop (right) structure is evident: the magnetic field is almost vertical at the points where the strongest Stokes V signals are (at the loop foot points) and is horizontal in the transition between one polarity and the other. Recently López Ariste et al. (2006a) have found U-loops in the photosphere below a filament structure by solving the  $180^\circ$  ambiguity inherent to the Zeeman effect, suggesting that these structures are at least allowed by the physics that drives the solar atmosphere. In our case, unfortunately, we do not have any observa-

<sup>1</sup> Stokes Inversion based on Response functions

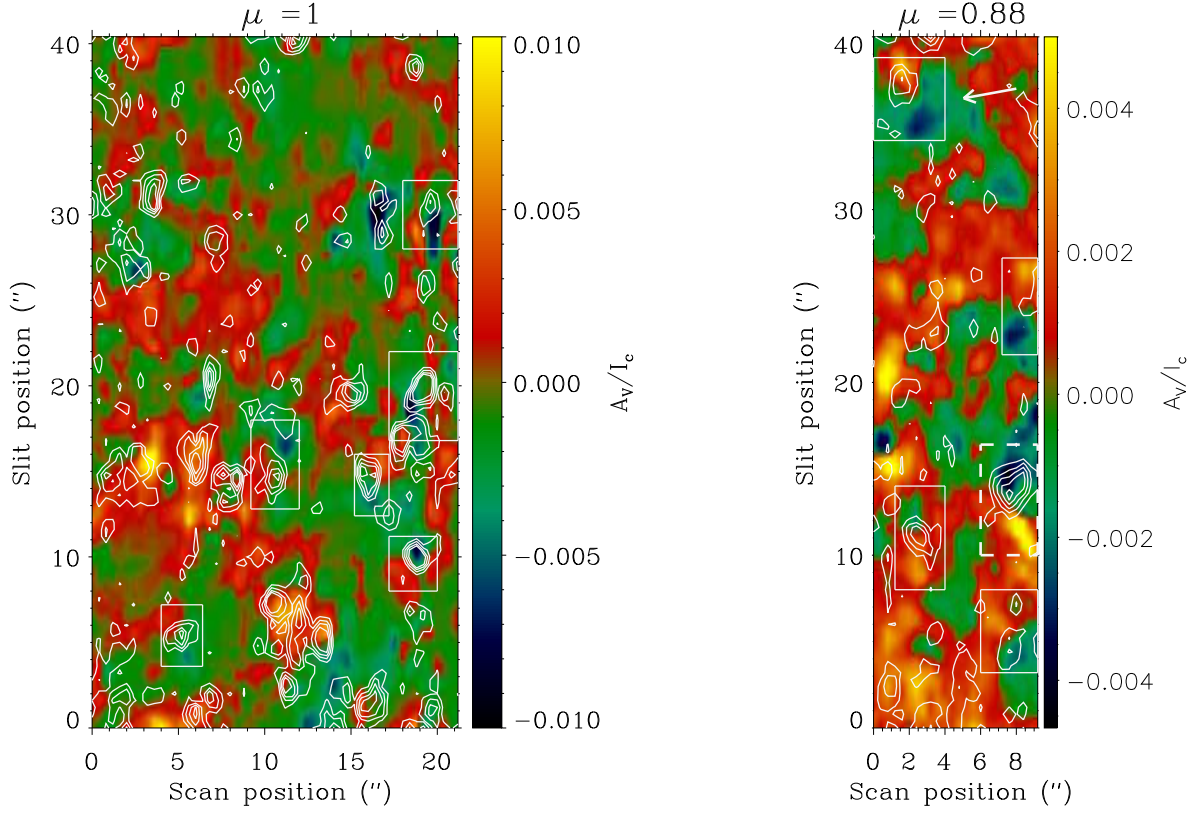


**Fig. 2.** Maps of the amplitude  $A_V$  of circular polarization (colour scale) of the observations taken at disc centre (left) and  $\mu = 0.88$  (right). The white contours represent the degree of linear polarization  $\sqrt{A_Q^2 + A_U^2}$  having the following values:  $1.5 \times 10^{-3}$ ,  $2 \times 10^{-3}$ ,  $2.5 \times 10^{-3}$ ,  $3 \times 10^{-3} I_c$  for the map at disc centre and additionally at  $1 \times 10^{-3}$  for the map at  $\mu = 0.88$ . The white arrow in the  $\mu = 0.88$  map points towards the position of the disc centre.

tional constraint to choose between the two different solutions showed in Fig. 3.

There are many bipolar regions potentially harboring low-lying loops in the maps in Fig. 2 but only those boxed in are as clear as the example shown in Fig. 3. This means that in all these cases the horizontal component of the magnetic vector is mainly directed along the line joining the opposite magnetic polarities and that the inclination is almost vertical in the foot points of the structure and rather horizontal in between. The observed loops are rather flat, with a foot point separation of 2300 km and with at least some of the field lines at the loop top lying in the height range of formation of the  $1.56 \mu\text{m}$  lines (i. e. only a few hundred km above the foot points). All cases also share some other properties. The magnetic field strength is weak, being below 500 G in the majority of the cases. There are only very few points reaching higher values as 800 – 1000 G.

The line of sight plasma flows in the magnetic atmosphere are correlated with the continuum intensity: bright structures in the continuum image are associated with upflows in the magnetic component, dark structures with downflows. The foot points of the magnetic structures are located equally probably in upflows or in downflows as seen in Fig. 4. The more vertical fields are located at the footpoints of the structure and we can see that they are found either in upflows or downflows. Also the more horizontal fields are lying both in upflows and downflows. This could be indicative of a dynamic scenario. If the time scale of the evolution of such structures is larger than the convective turnover time of granulation, one would expect  $\Omega$ -loops to be anchored in

intergranular lanes (where downflows dominate) and to be lying over granules. For U-loops the situation is expected to be reversed, however. Consequently, we may be seeing a mixture of  $\Omega$  and U-loops.

As seen in Fig. 3, the magnetic flux density of the selected loop has typical values of the internetwork. This is also true for the rest of the loops boxed in Fig. 2. The magnetic flux density in the pixels occupied by loops follow the same distribution as the pixels in the rest of the internetwork area. Also the magnetic field strength distribution is the same as that of the rest of the area covered by the typical internetwork. The fact that both the selected loops and the rest of the observed area share the same properties suggest that the internetwork could harbour many of these small low-lying loops, most of them remaining undetectable in our observations.

#### 4. Discussion and conclusions

We have detected 11 examples of low-lying (i. e. photospheric) loops in two scans of internetwork regions in the quiet Sun. These loops may be related to the horizontal features observed by Lites et al. (1996) and also the emerging flux in form of small bipoles observed by de Pontieu (2002) using the visible lines at 630 nm. In our case, we have more sensitive spectropolarimetric observations (very magnetically sensitive infrared lines and very low noise in both linear and circular polarization) which allow us to reconstruct the topology of the magnetic structures. Although we could not follow the evolution of such loop-like structures,

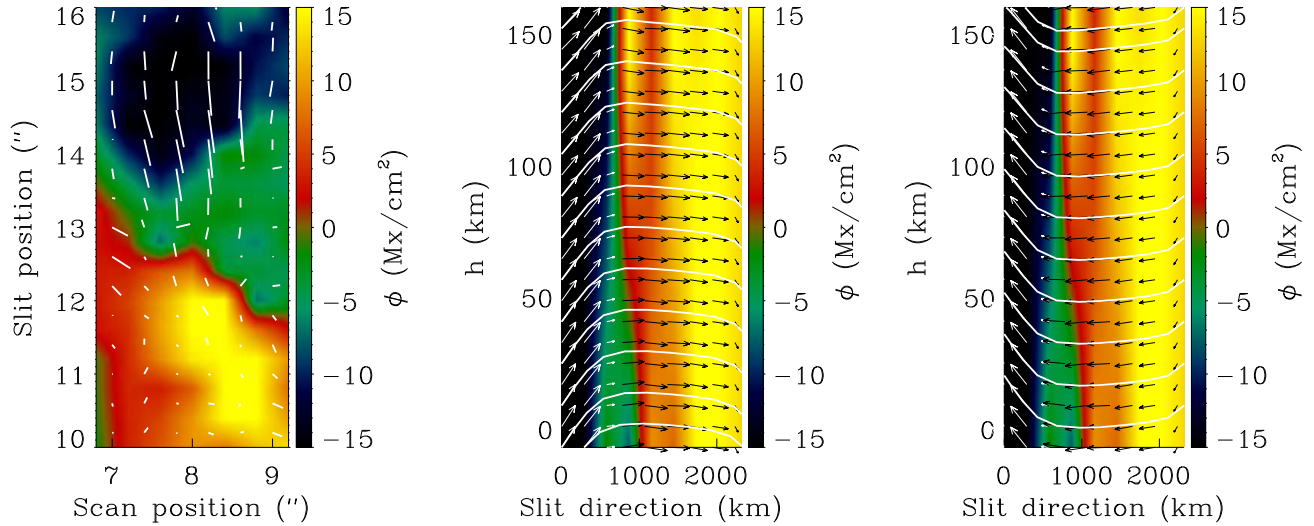


**Fig. 3.** Left panel: Map of the vertical magnetic flux density of the loop selected as an example (marked with a dashed square in the  $\mu = 0.88$  circular polarization map). The white lines represent the horizontal component of the magnetic flux vector. Centre and right panels: magnetic field lines computed for the two allowed magnetic field configurations, that differ by  $180^\circ$  in azimuth, giving rise to an  $\Omega$ - and a U-loop structure, respectively. The inclination and azimuth of the magnetic field vector have been translated to the local reference system.

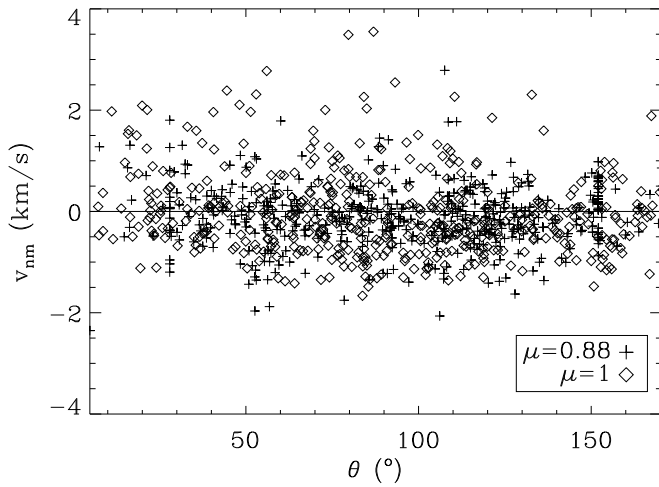


**Fig. 4.** Line-of-sight bulk velocity of the field free component plotted versus the inclination of the magnetic field inclination with respect to the local vertical. Positive values correspond to downflows and negatives to upflows.

one may speculate that the physical processes that give rise to these loops are small scale magnetic flux emergence in the internetwork quiet Sun.

Concerning the magnetic flux carried by the loop-like structures that we have identified, we find that at least 6.1% (disc centre) and 25.8% ( $\mu = 0.88$ ) of the magnetic flux in the whole map is emerging in the form of small scale magnetic loops. On average, this means that at least 10-20% of the magnetic flux in the solar internetwork is in the form of low-lying loops at any given time. This is a lower limit since further such features may have escaped detection due to the weakness of the associated linear polarization signals. One implication of the fact that these loops are so low-lying is that the magnetic flux they are con-

necting is unlikely to reach the chromosphere and higher layers. Unless we are observing a transient phase this implies that possibly much of the magnetic flux does not rise above the photosphere. This point deserves further attention in view of the suggestions of Trujillo Bueno et al. (2004) that a tangled field could provide the clue to understanding how the solar chromosphere and corona are heated.

**Acknowledgements.** This research has been funded by the Spanish Ministerio de Educación y Ciencia through project AYA2004-05792. Part of this work was done when M. J. Martínez González was visiting the Max Planck Institute in Lindau and she would like to express her gratitude to the staff for their warm hospitality. The authors acknowledge the comments of the anonymous referee which helped to improve the letter and strengthen the conclusions.

## References

- Asensio Ramos, A., Martínez González, M. J., López Ariste, A., Trujillo Bueno, J., & Collados, M. 2007a, *ApJ*, in press
- Asensio Ramos, A., Socas-Navarro, H., López Ariste, A., & Martínez González, M. J. 2007b, *ApJ*, in press
- Ballesteros, E., Collados, M., Bonet, J. A., et al. 1996, *A&A*, 115, 353
- Collados, M. 1999, in *Third Advances in Solar Physics Euroconference*, ed. B. Schmieder, A. Hofmann, & J. Staude, 184 (ASP Conference), 3–22
- Collados, M. V. 2003, in *Polarimetry in Astronomy*, ed. S. Fineschi, 4843 (Proceedings of the SPIE), 55–65
- de Pontieu, B. 2002, *ApJ*, 569, 474
- Faurobert, M., Arnaud, J., Vigneau, J., & Frisch, H. 2001, *A&A*, 378, 267
- Feldman, U., Widing, K. G., & Warren, H. P. 1999, *ApJ*, 522, 1133
- Keller, C. U., Deubner, F., Egger, U., Fleck, B., & Povel, H. 1994, *A&A*, 286, 626
- Khomenko, E. V., Collados, M., Solanki, S. K., Lagg, A., & Trujillo Bueno, J. 2003, *A&A*, 408, 1115
- Lin, H. 1995, *ApJ*, 446, 421
- Lin, H. & Rimmele, T. 1999, *ApJ*, 514, 448
- Lites, B. W., Leka, K. D., Skumanich, A. P., Martínez Pillet, V., & Shimizu, T. 1996, *ApJ*, 460, 1019
- López Ariste, A., Aulanier, G., Schmieder, B., & Sainz Dalda, A. 2006a, *A&A*, 456, 725
- López Ariste, A., Tomczyk, S., & Casini, R. 2006b, *A&A*, in press
- Manso Sainz, R., Landi Degl' Innocenti, E., & Trujillo Bueno, J. 2004, *ApJ*, 614, 89L
- Martínez González, M. J., Collados, M., & Ruiz Cobo, B. 2007, in *4th Solar Polarization Workshop*, ed. R. Casini & B. W. Lites, ASP Conference Series, in press

- Ruiz Cobo, B. & del Toro Iniesta, J. C. 1992, ApJ, 398, 375  
Schmidt, W. & Kentischer, T. 1995, A&A, 113, 363  
Solanki, S. K., Lagg, A., Woch, J., Krupp, N., & Collados, M. 2003, Nature, 425, 692  
Stenflo, J. O. 1987, Sol. Phys., 114, 1  
Trujillo Bueno, J., Shchukina, N., & Asensio Ramos, A. 2004, Nature, 430, 326